Proceedings of the 17th World Congress
The International Federation of Automatic Control
Seoul, Korea, July 6-11, 2008

Robust Adaptive Fault-Tolerant Control of the F-14 Aircraft under Sensor Failures ⋆

Sajjad Fekri * **Dawei Gu** * **Ian Postlethwaite** *
Michael Athans **

* *Control & Instrumentation Research Group, Department of Engineering, University of Leicester, U.K. (Tel: +44-116-2522567; Fax: +44-116-2522619; e-mail: {sf111,dag,ixp}@le.ac.uk)*
** *Institute for Systems and Robotics (ISR), Instituto Superior Técnico (IST), Lisbon, Portugal; also Professor of EE&CS (emeritus), MIT, Cambridge, MA, U.S.A. (e-mail: athans@isr.ist.utl.pt)*

Abstract: This paper presents a novel fault detection and isolation (FDI) architecture applied to the lateral-directional axis of an F-14 aircraft during powered approach to landing under sensor failures. The fault-tolerant architecture employed is based on the so-called "Robust Multiple-Model Adaptive Control" (RMMAC) and hence is referred to as "RMMAC/FDI". The results demonstrate successful stability and performance of the RMMAC/FDI architecture.

1. INTRODUCTION

In recent years, "fault detection and isolation" (FDI) strategies and "health monitoring control systems" (HMCS) for air vehicles have attracted considerable attention due to an increasing demand for appropriate technologies, systems, facilities, and procedures that will allow air vehicles to operate safely and routinely.

The main purpose of an FDI scheme is to generate an alarm when a fault occurs (detection), and then to determine the location of the fault (isolation), so that corrective action or preventive measures can be taken to eliminate or minimize the effect of the fault; see Patton *et al.* [1989].

Control systems designed for aircraft must be capable of tolerating normal as well as failure conditions whilst still maintaining guaranteed stability-robustness and desirable performance robustness. Fault tolerance is of particular importance in realistic applications where the environment, system parameters, and failure parameters change abruptly or incipiently and hence there is a requirement on the system to be robust to these uncertainties, see e.g. Barrett *et al.* [1996].

Control reconfiguration is a building block towards an increasing dependability of feedback control systems and an active approach to achieve fault-tolerant control for dynamic systems; it is used when severe faults, such as actuator or sensor outages, cause a break-up of the control loop, which must be restructured to prevent failure at the system level and hence must be robust to accommodate changed plant dynamics; see Patton [1997].

⋆ This work was co-funded by the Technology Strategy Board's Collaborative Research and Development programme (following an open competition), BAE Systems and EPSRC, UK.
The Technology Strategy Board is an executive body established by the Government to drive innovation. It promotes and invests in research, development and the exploitation of science, technology and new ideas for the benefit of business - increasing sustainable economic growth in the UK and improving quality of life.

If system faults are ignored for a long time, they may cause catastrophic and disastrous effects, such as loss of human life, economic collapse, environmental pollution, and so on. Therefore, it would be of great interest to detect such faults immediately. In cases the consequences of a fault are not very severe, early detection of faults can help improve efficiency, productivity, reliability, and cost financial; see Tan [2002].

There are two main methods for FDI: hardware redundancy and analytical redundancy. In FDI schemes based on hardware redundancy, most flight control laws are implemented with a redundant set of computers in such a manner that the control system is fault tolerant. Fault tolerance implies that one or more of the channels can fail with no degradation in control system performance. However, such FDI methods may not always be physically and financially feasible; additional sensors incur additional costs, occupy more space, and cause the system to be heavier; see U.S. National Research Council [2006].

An analytical redundancy based FDI scheme requires a model which is usually a linear approximation of the actual system about a certain operating point, and therefore, is not a completely accurate representation of the system. In obtaining the model, some of the dynamics could have been neglected, approximations will have been used and estimates of certain parameters made. This results in a mismatch between the model and the actual system. In modelling terms this discrepancy is accounted for by the introduction of a class of uncertainty. An advantage of such FDI method is that a minimal number of sensors are needed. However, a good model of the system (describing the input-output relationship) is required– hence, an analytical redundancy FDI is also known as "model based FDI". What if the model dynamics are not described precisely or include large uncertain real parameters due to physical changes in the plant and occurrence of failures? The answer is to use an FDI scheme that is robust to model

978-1-1234-7890-2/08/$20.00 © 2008 IFAC 10.3182/20080706-5-KR-1001.1453

uncertainty by producing residuals which are sensitive to the faults but insensitive to the uncertainties.

If the plant under investigation is subject to the time-varying parameters due to the failures, the performance achieved by any "robust non-adaptive FDI design" may be abysmal. In such cases, we must use some sort of "robust adaptive FDI design" to obtain a "graceful performance".

In this paper, we shall focus upon "robust performance" requirements on the "robust adaptive" FDI design implemented by one of the available multiple-model methods. We follow the recent research on "Robust Multiple-Model Adaptive Control (RMMAC)", see Athans *et al.* [2005], Fekri [2006], and extend it to a new analytical redundancy robust FDI scheme, which is referred to as "RMMAC/FDI" design, to study a preliminary design and testing of a "self-repairing robust multivariable FDI method" focusing on an F-14 aircraft. The fault scenarios under consideration are sensor faults. Actuator faults will not be discussed in this paper due to space limitations.

The rest of the paper is organized as follows. Some of the concepts and outstanding issues of RMMAC and RMMAC/FDI methodologies are overviewed in Section 2. In Section 3 we describe the dynamics of the lateral-directional axis of an F-14 aircraft during powered approach to landing and in Section 4 we consider the design of robust controllers. Simulation results are presented in Section 5. Section 6 summarizes our conclusions.

2. THE RMMAC/FDI METHODOLOGY

The general philosophy of the RMMAC introduced in Fekri *et al.* [2004] was to tackle the problem of stability- and performance-robustness for LTI uncertain plants subject to uncertain real parameters (possibly large) and unmodelled dynamics. Space limitations preclude including the details– more technical detail on the general RMMAC structure are found in Athans *et al.* [2005], Fekri [2006], Fekri *et al.* [2006].

Similarly, the RMMAC/FDI architecture integrates robust controller synthesis, using the mixed-μ synthesis method (Balas *et al.* [2007]), with dynamic hypothesis-testing concepts using explicit robust-performance requirements for the adaptive design that quantifies the adaptive performance improvement.

The RMMAC based fault-tolerant architecture (RMMAC/FDI) is shown in Figure 1 which represents a new variant in the class of multiple-model adaptive fault-tolerant schemes. The RMMAC/FDI architecture, as shown in Figure 1, is based on a bank of $N + 1$ steady-state discrete-time Kalman filters (KFs) where KF#0 is associated with normal operation (no failure) and KF#1, . . . ,KF#N are associated with particular status of the system failures, to ensure that the identification subsystem converges to the "nearest probabilistic neighbour" in order to detect fault occurrence correctly. These Kalman filters are part of the "failure identification subsystem".

The number of models employed in the RMMAC/FDI architecture $(N + 1)$ is a natural byproduct of performance requirements imposed on this "self-repairing adaptive system". Once the number of models is fixed, $N + 1$

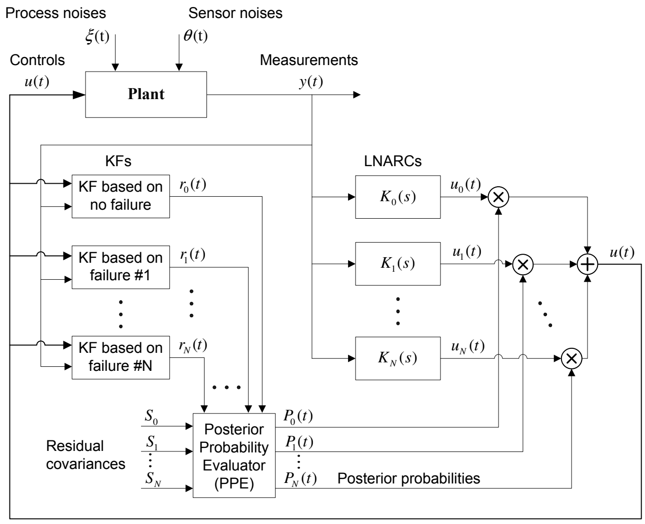

Fig. 1. The RMMAC/FDI architecture

compensators of the RMMAC/FDI, which are so-called "Local Non-Adaptive Robust Compensators (LNARCs)", are designed using the mixed-μ synthesis methodology, see Fekri [2006]. LNARC#0 (or $K_0(s)$) is, in essence, a robust compensator designed for the normal operation model (Model#0) and $K_1(s), \ldots, K_N(s)$ are robust compensators designed for failure models, all with the best possible (and guaranteed) stability- and performance-robustness albeit with an "inherent degradation in performance" for failure models Model#1, . . . ,Model#N.

The KF residuals drive the "Posterior Probability Evaluator (PPE)" that generates a set of posterior probabilities that indicate which failure model is the "closest" model to the actual system in the probabilistic sense. Under suitable assumptions, one of the posterior probabilities will converge to unity, i.e. detect the most likely failure model. The overall adaptive FDI is then generated by the probabilistic weighting of the local controls generated by the bank of compensators, see Fekri [2006].

An advantage of the RMMAC/FDI architecture is that its FDI asymptotic performance can be predicted, either in the frequency domain (using sensitivity singular value plots) or in a stochastic setting (using RMS values).

3. F-14 LATERAL DYNAMICS

In this section, we discuss the modelling of the lateral-directional axis of an F-14 aircraft during powered approach to landing. The RMMAC/FDI designed for this aircraft includes nine models, one model for normal operation and eight models for sensor failures on the roll rate and the yaw rate measurements, as well as nine robust controllers designed using mixed-μ synthesis for the normal operation model and eight failure models, respectively.

3.1 Nominal F-14 Aircraft Model

The linearized lateral F-14 model is derived at an angle-of-attack of 10.5 degs and airspeed of 140 knots; the reader is referred to G.J. Balas *et al.* [1996] for a detailed derivation of this model. The pilot commands the lateral-directional response of the aircraft with the lateral stick and rudder pedals. The aircraft has the following attributes:

I) Two control inputs: differential stabilizer deflection (δ_{dstab}, degs) and rudder deflection (δ_{rud}, degs).

II) Three measured outputs: roll rate (p, deg/sec), yaw rate (r, degs/sec), and lateral acceleration (y_{ac}, g's).

III) One calculated output: side-slip angle (β).

The nominal lateral directional F-14 model has four states: lateral velocity (v), yaw rate (r), roll rate (p), and roll angle (ϕ). These variables are related by the continuous-time model $\bar{G} = \left[\begin{array}{c|c} A & B \\ \hline C & D \end{array}\right]$, described by the following state space equations:

$$\begin{aligned} \dot{x}(t) &= Ax(t) + Bu(t) \\ y(t) &= (I + \Delta_S)Cx(t) + Du(t) + \theta(t) \end{aligned} \tag{1}$$

where

$$A = \begin{bmatrix} -0.116 & -227.3 & 43.02 & 31.63 \\ 0.00265 & -0.259 & -0.1445 & 0 \\ -0.02114 & 0.6703 & -1.365 & 0 \\ 0 & 0.1853 & 1 & 0 \end{bmatrix}$$

$$B^T = \begin{bmatrix} 0.062205 & -0.005252 & -0.046664 & 0 \\ 0.101265 & -0.011212 & 0.003644 & 0 \end{bmatrix}$$

$$C = \begin{bmatrix} 0.2469 & 0 & 0 & 0 \\ 0 & 0 & 57.3 & 0 \\ 0 & 57.3 & 0 & 0 \\ -0.002827 & -0.007877 & 0.05106 & 0 \end{bmatrix}$$

$$D^T = \begin{bmatrix} 0 & 0 & 0 & 0.002886 \\ 0 & 0 & 0 & 0.002273 \end{bmatrix}$$

and $x^T = [v \quad r \quad p \quad \phi]$ is the state vector, $u^T = [\delta_{dstab} \quad \delta_{rud}]$ is the control vector, and $y^T = [\beta \quad p \quad r \quad y_{ac}]$ is the measurement vector. $\Delta_S = \mathrm{diag}(0, \sigma_p - 1, \sigma_r - 1, 0); \sigma_p, \sigma_r \in [0.5, 1.5]$ is the sensor fault uncertainty block.

It is worthwhile to emphasize again that failures are considered only at one or two sensors (on the roll rate and the yaw rate measurements). Note that under normal operation $\Delta_S = 0_{4\times 4}$ but, for the failure models, the values of σ_p and σ_r are considered as in Table 1.

The performance of the control system are taken to be $z^T = [\beta \quad p]$ variables as

$$z(t) = C_p x(t) \tag{2}$$

where

$$C_p = \begin{bmatrix} 0.2469 & 0 & 0 & 0 \\ 0 & 0 & 57.3 & 0 \end{bmatrix}$$

Without loss of generality, plant disturbances in the F-14 dynamics concatenated with the aircraft model are not considered. Such disturbance modelling might consider or be similar to a Dryden gust model to quantify the impact of gusts on aircraft performance; see Barrett *et al.* [1996].

The frequency range is selected as $\omega \in [0.01, 100]$ rad/sec which captures all the dynamics of the weighted interconnection structure.

The complete airframe model also includes actuator models $A_S = \mathrm{diag}(\frac{25s}{s+25}, \frac{25}{s+25})$ and $A_R = A_S$. The actuators outputs are their respective rates and deflections. The actuator rates are used to penalize the actuation effort.

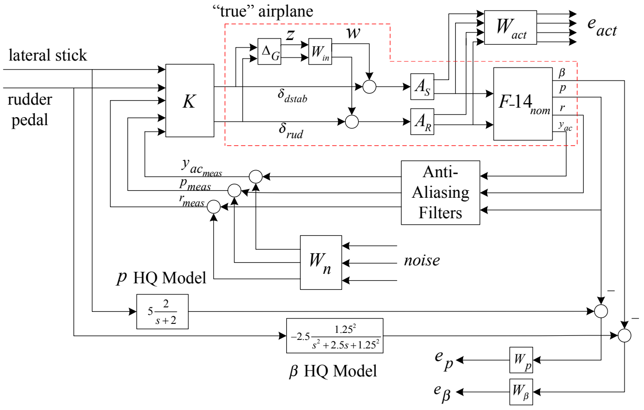

Fig. 2. Robust Control Design for F-14 Lateral Axis

Since the nominal F-14 model, $\bar{G}$, only approximates true airplane behaviour (there are usually approximations in the nonlinear equations from which the linear equations are derived), we shall introduce a relative term or multiplicative uncertainty $W_{in}\Delta_G$ at the plant input, to account for unmodelled dynamics, so that the true airplane dynamic would be

$$G = (I + W_{in}\Delta_G)\bar{G} \tag{3}$$

The set of such models selected for control design could represent uncertainties associated with the approximations in aerodynamics, structural dynamics, and actuator and sensor dynamics. Here, the error dynamics Δ_G have gain less than 1 across frequencies, and the weighting function W_{in} reflects the frequency ranges in which the model is more or less accurate. There are typically more modelling errors at high frequencies so W_{in} is high pass and selected as $w_1 = \frac{2.0(s+4)}{s+160}$ and $w_2 = \frac{1.5(s+20)}{s+200}$.

By quantifying modelling errors as above, we can now build an uncertain model of the aircraft dynamics using the nominal airframe model and the actuator models A_S and A_R, as shown in Figure 2 with the dashed box.

3.2 F-14 Sensor Faults

The lateral F-14 control system includes three measured outputs on roll rate p, yaw rate r, and lateral acceleration y_{ac}. The most important measurements which are dominant when a sensor fault occurs, and considered in this paper, are the measurements on roll rate and yaw rate.

The nine models were employed in the RMMAC/FDI design including the "no failure" model (Model#0), as shown in Table 1. In this table, "NO" stands for no failure i.e. $\sigma_p = \sigma_r = 1$, "UE" stands for faults with 50%-100% loss of measurement accuracy (under-estimated) i.e. $\sigma_p, \sigma_r \in [0.5, 1]$, and "OE" stands for faults with 100%-150% loss of measurement accuracy (over-estimated), i.e. $\sigma_p, \sigma_r \in [1, 1.5]$.

4. ROBUST LATERAL-AXIS CONTROLLERS

Next we shall proceed with designing controllers that robustly achieve the specifications, where robustly for the nominal operation controller, $K_0(s)$, means for any perturbed aircraft model consistent with the modelling

Table 1. Normal operation (no failure) and sensor failure parameters

M#	0	1	2	3	4	5	6	7	8
σ_p	NO	NO	NO	UE	UE	UE	OE	OE	OE
σ_r	NO	UE	OE	NO	UE	OE	NO	UE	OE

NO (Normal Operation): $\sigma_p = \sigma_r = 1$
UE (Under-Estimated measurements): $\sigma_p, \sigma_r \in [0.5, 1]$
OE (Over-Estimated measurements): $\sigma_p, \sigma_r \in [1, 1.5]$

error bounds W_{in}, see Balas *et al.* [2007]. For the failure operation controllers, $K_1(s), \ldots, K_8(s)$, robustly means modelling error bounds W_{in} as well as uncertain real parameters σ_p and σ_r due to the sensor failures.

The block diagram of the closed-loop system, as shown in Figure 2, includes the nominal aircraft model, the controller $K(s)$, as well as elements capturing the model uncertainty and performance objectives.

The control system design goal is to have the "true" airplane respond effectively to the pilot's lateral stick and rudder pedal inputs. These performance specifications include:

1) Decoupled responses from lateral stick to roll rate p and from rudder pedals to side-slip angle β. The lateral stick and rudder pedals have a maximum deflection of ± 1 inch.

2) We judge handling qualities (HQ) by comparing closed-loop-system frequency responses with those of low-order transfer functions. Here, the aircraft handling quality response from lateral stick to roll rate p should match the first-order response $hq_p = 5.0\frac{2.0}{s+2.0}$. The aircraft handling quality response from the rudder pedals to the side-slip angle β should match the damped second-order response $hq_\beta = -2.5\frac{1.25^2}{s^2+2.5s+1.25^2}$.

3) The stabilizer actuators have ± 20 degs and ± 90 degs/sec limits on their deflection and deflection rate. The rudder actuators have ± 30 degs and ± 125 degs/sec deflection and deflection rate limits.

4) The three measurement signals (roll rate p, yaw rate r, and lateral acceleration y_{ac}) are filtered through second-order anti-aliasing filters $AF_p(s) = \frac{1300.72}{s^2+36.06s+1300.72}$, $AF_r(s) = \frac{6168.5}{s^2+78.54s+6168.5}$, and $AF_l(s) = \frac{6168.5}{s^2+78.54s+6168.5}$.

4.1 Weighting functions

To apply the mixed-μ synthesis tool, we first must recast our design tradeoffs and frequency-dependent specifications as constraints on the closed-loop gains. We shall use weighting functions to "normalize" our specifications across frequency and to weight each requirement adequately for all controllers of Figure 1. We shall express the F-14 specifications in terms of weighting functions:

a) To capture the limits on the actuator deflection magnitude and rate, pick a diagonal, constant weight, such as W_{act}, corresponding to the stabilizer and rudder deflection rate and deflection limits, i.e. $W_{act} = \text{diag}(\frac{1}{90}, \frac{1}{20}, \frac{1}{125}, \frac{1}{30})$.

b) We can use a 3×3 diagonal, high-pass filter W_n to model the frequency content of the sensor noise in the roll rate, yaw rate, and lateral acceleration channels, i.e. $W_n(s) = \text{diag}(0.025, \frac{0.0125(s+1)}{s+100}, 0.025)$.

c) The lateral stick-to-$|p|$ and rudder pedal-to-$|\beta|$ responses should match the handling quality targets hq_p and hq_β. This is a model-matching objective i.e. to minimize the difference (peak gain) between the desired and actual closed-loop transfer functions. Performance is limited due to a right-half plane zero in the model at 0.0246 rad/sec, so accurate tracking of sinusoids below 0.0246 rad/sec is not possible. Accordingly, we shall weight the first handling quality spec with a bandpass filter $W_p(s) = \frac{0.06s^4+3.42s^3+125s^2+7.28s+0.188}{s^4+9.19s^3+30.80s^2+18.83s+3.95}$ that emphasizes the frequency range between 0.06 and 30 rad/sec; we prefer a roll rate tracking error of less than 6%. Figure 3 shows the "best" performance weight in the frequency domain that we used for the normal operation model.

Similarly, for the second handling quality specifications we choose $W_\beta = 2W_p$.

The above weights will be considered in the subsequent controller design using mixed-μ synthesis for the "no failure" model (normal operation) as the reference. After occurrence of a fault, it is important to know if the original system performance can be recovered or we should accept some degree of performance degradation. Towards this end, we shall introduce a performance gain, A_p, for all failure models so that the new performance weights are considered as

$$\begin{aligned} W_p^f &= A_p \cdot W_p \\ W_\beta^f &= A_p \cdot W_\beta \end{aligned} \tag{4}$$

where the performance gain, A_p, would take such performance degradation into account in the design process.

4.2 Design of lateral-axis controllers using μ -synthesis

By constructing the weighting functions W_{act}, W_n, W_p, and W_β according to the previous section, a μ controller for normal operation meets the specifications whenever the upper bound of μ satisfies

$$\mu_{u.b.} \leq 1.0 \tag{5}$$

at all frequencies and for any I/O directions. When designing the μ controllers we have used $0.99 \leq \mu_{u.b.} \leq 1.0$ so that whenever, at the "best" iteration among all iterations, this condition is satisfied, we have reached the "best" local μ controller associated with the specific failure scenario.

Next, using mixed-μ synthesis, eight "local" robust compensators, $K_1(s)$, $K_2(s), \ldots, K_8(s)$, are designed for eight failure models defined in Table 1. In mixed-μ synthesis, the weights W_{act} and W_n are similar to those used in the

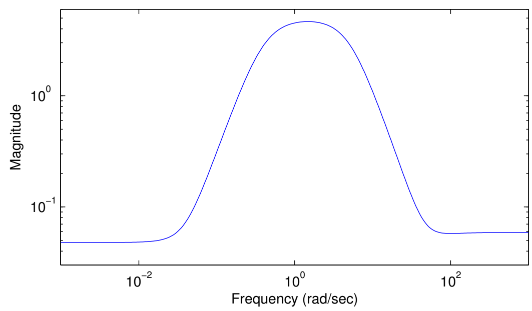

Fig. 3. 'Performance weight used in subsequent design for the aircraft normal operation model (no failure).

normal operation design. However, for each failure control system design, the performance gain (A_p) in eq. (4) is decreased until the μ upper-bound in eq. (5) is achieved.

Table 2 shows the "best" performance gains for the normal operation and eight failure models illustrating how much the level of flight performance will degrade from that of normal operation if sensor faults occur in sensors. Hence, in the presence of fault, how system sacrifices performance to yield an "acceptable performance degradation" to guarantee its stability, becomes a predominant issue. This "performance degradation" due to the loss of measurement accuracy is very important for implementing any fault-tolerant control system.

4.3 Design of discrete-time Kalman filters

The bank of discrete-time Kalman filters in the RMMAC/FDI structure is required as the fault identification subsystem and is designed next. The reader is referred to e.g. Gelb [1974] for a detailed derivation of the Kalman filter. The nine models for the Kalman filters (KFs) are chosen based on nominal points as shown in Table 3.

It is emphasized that the "fake plant white noise", Ξ_f, is included for the purpose of preventing the fault identification subsystem of the RMMAC/FDI from being overconfident in its estimates and not switching to a different model rapidly due to the occurrence of different faults. In fact, the need for such fake-plant-white-noise is to compensate for the (large) unknown failure parameters, σ_p, σ_r, within each KF so as to increase the KFs gains to pay more attention to the information contained in residual signal.

The following fake-white-noise intensities were found suitable for the failure models considered here:

$$\Xi_f = \text{diag}\{5\times10^{-4}\,,\ 0\,,\ 2\times10^{-3}\,,\ 0\,,\ 0\,,\ 0\,,\ 0\,,\ 0\,,\ 0\} \quad (6)$$

The non-zero disturbance intensities in eq. (6) appear upon the equations $\dot{x}_1(t)$ and $\dot{x}_3(t)$ that are essential due to the sensor fault uncertainties at failure models.

5. SIMULATION RESULTS

In this section, we present some stochastic simulations using the complete RMMAC/FDI architecture. Of course, testing such a robust adaptive FDI technique requires significant computations using multiple Monte Carlo (MC) runs under different fault scenarios. Due to space limitations, only representative plots are shown; however, our conclusions are based on many other MC runs not explicitly shown in this paper.

Here, the normal operation design is briefly called "non-adaptive" while the RMMAC/FDI design is called "adaptive". We shall compare the performance achieved by the non-adaptive design with that of the RMMAC/FDI design. Recall that the performance specifications are achieved when inequality (5) is satisfied at every frequency.

Table 2. Best performance gains under normal/failure operations

Model#	0	1	2	3	4	5	6	7	8
A_p	1	0.34	0.33	0.22	0.1	0.1	0.23	0.1	0.1

Table 3. The nominal parameters of Kalman filters (KFs) used in the RMMAC/FDI

KF#	0	1	2	3	4	5	6	7	8
σ_p^*	1.00	1.00	1.00	0.75	0.75	0.75	1.25	1.25	1.25
σ_r^*	1.00	0.75	1.25	1.00	0.75	1.25	1.00	0.75	1.25

$\sigma_p^*(i)$ and $\sigma_r^*(i)$ are the nominal failure parameters used in Model#i associated with KF#i.

In all the responses below, the stick/rudder input is a 1.0 inch doublet pair as shown in Figure 4.

Also, in this set of simulations, we have assumed that the sequences of sensor faults (due to loss of accuracy arising from over- and under-estimated measurements) occur sinusoidally on the roll rate and the yaw rate sensors as shown in Figure 5.

Figure 6 show the time-evolution of the posterior probabilities $P_0(t), P_1(t), P_6(t)$, and $P_7(t)$ generated by the PPE. All probabilities were initialized by $P_k(0) = 1/9$, $k = 0, 1, \ldots, 8$. These probabilities have followed the "correct" failure sequences of Figure 5; see Table 1. The other five probabilities (not shown) decay rapidly from their initial values of 1/9 to zero. Figure 7 shows the aircraft performance output under the sensor failure sequences shown in Figure 5. Both the closed-loop responses are almost

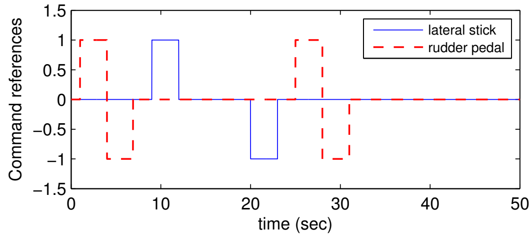

Fig. 4. Lateral stick and rudder pedal command inputs.

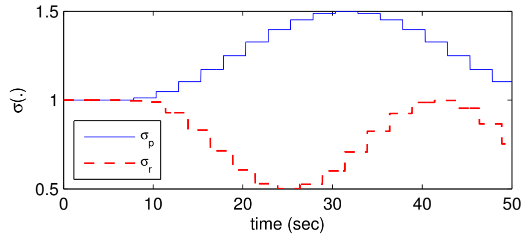

Fig. 5. Failure parameters of the sensors: σ_p and σ_r, respectively, for the roll rate and the yaw rate sensors.

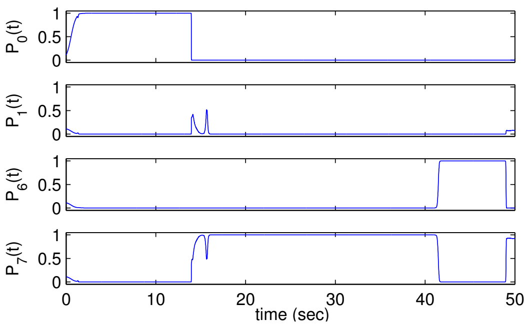

Fig. 6. Transient behaviour of RMMAC/FDI posterior probabilities.

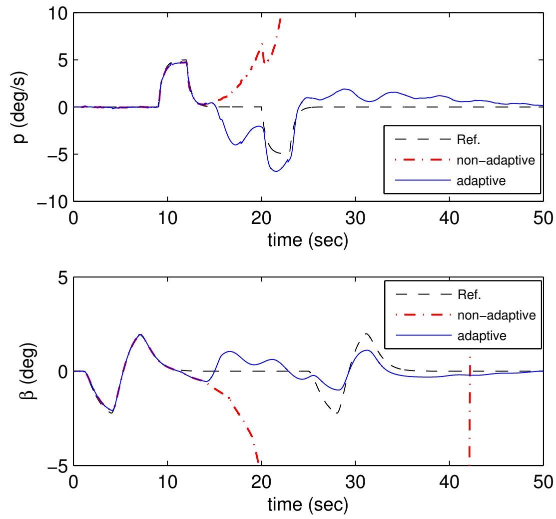

Fig. 7. Comparison of the performance outputs.

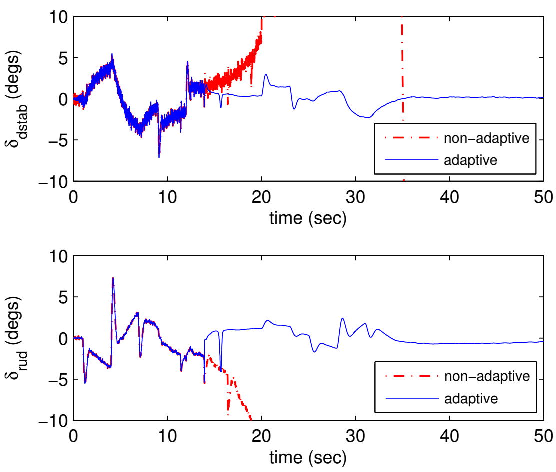

Fig. 8. Differential stabilizer deflection (δ_{dstab}, degs) and rudder deflection (δ_{rud}, degs).

identical, for the non-adaptive and the RMMAC/FDI designs before about $t = 14$ secs. However, after $t = 14$ secs, the non-adaptive design is unstable while RMMAC/FDI remains stable albeit with a degraded performance, as expected in Table 2.

The control signals (differential stabilizer and rudder deflections) are shown in Figure 8. It is worthwhile to note that, before occurrence of sensor faults starting at $t = 10$ secs (see Figure 5), both control signals used by non-adaptive and adaptive designs are identical. However, after occurring faults, the RMMAC/FDI design stabilizes the aircraft and outperforms the non-adaptive FDI design.

Similar stochastic Monte Carlo simulations (not shown) were made for a variety of cases including constant and time-varying sensor failures in which RMMAC/FDI was able to detect them and reconfigure the aircraft control system successfully. Besides, all those results were consistent with the reduced performance implied by Table 2.

6. CONCLUSIONS

How an aircraft survives with an acceptable performance degradation and how to explicitly incorporate allowable system performance degradation in the design process in the event of faults are very important issues.

This paper explains the importance of an adaptive FDI scheme by presenting a novel "Robust FDI scheme" using "RMMAC/FDI". The RMMAC/FDI architecture uses frequency domain tools providing system designers clear rules for establishing when robust adaptive FDI architectures are required and, if required, how to design them by resorting to techniques that are extremely useful to the FDI problems. The RMMAC/FDI architecture is very flexible and hence increasingly can be applied in many reconfigurable FDI applications. The simulation results used several different fault scenarios including time-varying fault consequences demonstrating stability and performance properties of the RMMAC/FDI design as compared to the "best non-adaptive robust FDI scheme".

REFERENCES

M. Athans *et al.* Issues on robust adaptive feedback control. In *Invited plenary paper, In Preprints of 16th IFAC World Congress*, pages 9–39, Prague, Czech Republic, July 2005.

G.J. Balas *et al.* *Robust Control Toolbox, User's Guide.* The MathWorks Inc., Natick, MA, Sep. 2007.

M. Barrett *et al.* Application of multivariable control theory to aircraft control laws. Technical report, Honeywell Technology Center, Minneapolis, MN; Lockheed Martin Tactical Aircraft Systems, Ft. Worth, Texas: and Lockheed Martin Skunk Works, Palmdale, CA, 1996.

S. Fekri. *Robust adaptive MIMO control using multiple-model hypothesis testing and mixed-μ synthesis.* PhD thesis, Instituto Superior Técnico, Lisbon, Portugal, Jan. 2006.

S. Fekri *et al.* RMMAC: A novel robust adaptive control scheme – Part I: Architecture. In *Proc. of the IEEE Conf. on Decision and Control*, pages 1134–1139, Paradise Island, Bahamas, Dec. 2004.

S. Fekri *et al.* Issues, progress, and new results in robust adaptive control. *Int. J. of Adaptive Control and Signal Processing*, 20(10):519–579, Dec. 2006.

A. Gelb. *Applied Optimal Estimation.* MIT Press, MA, USA, 1974.

G.J. Balas *et al.* Design of controller for the F-14 aircraft lateral-directional axis during powered-approach. In *Proceedings of the AIAA Guidance, Navigation and Control Conference*, San Diego, CA, Paper No. AIAA-96-3781, July 1996.

R.J. Patton. Fault-tolerant control: the 1997 situation. In *Preprints of IFAC Symposium on Fault Detection Supervision and Safety for Technical Processes*, Kingston upon Hull, UK, 1997.

R. Patton *et al.* *Fault Diagnosis in Dynamic Systems : Theory and Application.* Prentice Hall, Nov. 1989.

C.P. Tan. *Sliding mode observers for fault detection and isolation.* PhD thesis, University of Leicester, Leicester, UK, 2002.

U.S. National Research Council. *Decadal Survey of Civil Aeronautics: Foundation for the Future.* National Academy Press, June 2006.